Biochemical and Biophysical Research Communications 408 (2011) 559–565

Contents lists available at ScienceDirect

Biochemical and Biophysical Research Communications

journal homepage: www.elsevier.com/locate/ybbrc

Cloning and heterologous expression of new xANO2 from *Xenopus laevis*

Rae Hyung Ryu [a], Soo Jin Oh [b], Ra Mi Lee [a], Seong Won Jeong [a], Lily Yeh Jan [c], Chi Ho Lee [d], C. Justin Lee [b], Sang Min Jeong [a,*]

[a] Department of Biochemistry and Molecular Cell Biology, College of Veterinary Medicine, Konkuk University, 1 Hwayang-dong, Gwangjin-gu, Seoul 143-701, Republic of Korea
[b] Neuroscience Program, The University of Science and Technology, 39-1 Hawolgokdong, Seongbukgu, Seoul 136-791, Republic of Korea
[c] Department of Physiology, Howard Hughes Medicine Institute, University of California, San Francisco, CA 94143, USA
[d] College of Animal Bioscience and Technology, Konkuk University, 1 Hwayang-dong, Gwangjin-gu, Seoul 143-701, Republic of Korea

ARTICLE INFO

Article history:
Received 9 April 2011
Available online 20 April 2011

Keywords:
Xenopus laevis
Anoctamin gene
Calcium-activated chloride channel
Tissue distribution
Heterologous expression

ABSTRACT

We have successfully isolated a novel anoctamin (xANO2), Ca^{2+}-activated chloride channel (ANO1, TMEM16A), from *Xenopus laevis*. The cDNA sequence was determined to belong to the anoctamin family by comparison with the xTMEM16A sequence in a previous report. Full length cDNA synthesis was performed by repeating 5′- and 3′-rapid amplification of cDNA end (RACE). We successfully completed the entire cDNA sequence and transiently named this sequence xANO2. The xANO2 cDNA is 3884 base pair (bp) long and codes 980 amino acid (aa) proteins. According to an aa homology search using the Basic Local Alignment Search Tool (BLAST), xANO2 showed an overall identity of 92% to xTMEM16A (xANO1) independently sub-cloned in our laboratory. A primary sequence of xANO2 revealed typical characteristics of transmembrane proteins. In tissue distribution analysis, the gene products of anoctamins were ubiquitously detected by real-time PCR (RT-PCR). The expression profiles of each anoctamin were different among brain, oocytes, and digestive organs with relatively weak expression. To clarify the anoctamin activity, physiological studies were performed using the whole cell patch-clamp technique with HEK293T cells, enhanced green fluorescent protein (EGFP), and expression vectors carrying anoctamins. Characteristics typical of voltage-dependent chloride currents were detected in cells expressing both xANO2 and xTMEM16A but not with EGFP alone. Sensitive reactions to the anion channel blocker niflumic acid (NFA) were also revealed. Considering these results, xANO2 was regarded as a new TMEM16A belonging to the *Xenopus* anoctamin family.

1. Introduction

Recently, TMEM16A was characterized and reported as a calcium-activated chloride channel (CaCC) in *Xenopus laevis* [1]. Even though the TMEM16A gene is regarded as a CaCC in higher animals [2–4], many also have another type of CaCC family known as chloride channels calcium activated (CLCA) [5–10]. The CLCA gene family has been studied in a number of tissues including the central nervous system, endothelial cells, smooth muscle, and secretory epithelial cells [8,11–14]. These genes are reported to play important physiological roles in the function of epithelial secretion, repolarization of cardiac action potential, regulation of vascular tone, olfactory transduction, neuronal excitability, and cell–cell adhesion [14].

In contrast to the CLCA family, little is known regarding the function of the CaCC TMEM16 family. In spite of similar functional characteristics such as Ca^{2+}-activated chloride conductance, there are no other similarities between CLCAs and TMEM16A. It has recently been shown that some proteins of the mammalian TMEM16 family, such as TMEM16A, may aid in the development of CLCA modulators for treating diseases such as hypertension and cystic fibrosis [1,15]. Also, Jason et al. used the first knockout of a vertebrate TMEM16 family member in a mouse model of tracheomalacia. Following analysis of their mutant mouse experimental results, they proposed that TMEM16A could be a novel regulator of epithelial and smooth muscle cell formation in murine development [16].

Much diverse research has been performed to identify the molecular characteristics of CLCA family members, but the mammalian species investigated have been limited [11–14,17]. We previously reported the cloning and functional expression of rbCLCA1 [8] from rat brain which was 82% identical to mCLCA1 [6]. The demand for genetic information from various animal species has increased, and still little is known regarding *X. laevis*; therefore, we began to identify the anion channels of *X. laevis*. The purpose of this study was to isolate a novel CaCC in *X. laevis*. Here, we introduce a novel anoctamin gene of *Xenopus* and describe its functional expression *in vitro*.

* Corresponding author. Fax: +82 2 450 3704.
E-mail address: jeongsm@konkuk.ac.kr (S.M. Jeong).

0006-291X/$ - see front matter © 2011 Elsevier Inc. All rights reserved.
doi:10.1016/j.bbrc.2011.04.060

2. Materials and methods

2.1. Materials

Molecular reagents were purchased from Takara Korea (Seoul, Korea), iNtRON Biotechnology (Seongnam, Korea), Toyobo (Osaka, Japan), Invitrogen (San Diego, CA, USA), QIAGEN (Valencia, CA, USA), Amersham Biosciences (Buckinghamshire, England) and BD Biosciences (Franklin Lakes, NJ, USA). The pGEM®-T Easy Vector was ordered from Promega (Madison, WI, USA). DyNAmo Flash® SYBR Green qPCR Kits (Finnzymes Oy, Espoo, Finland) were ordered from PharmaTech Co. A CHROMO4™ real-time PCR system was purchased from BIO-RAD (Hercules, CA, USA). All other chemical reagents were purchased from BioPure (Burlington, Ontario, Canada). *X. laevis* TMEM16A plasmid was provided by Professor L.Y. Jan (University of California, CA, USA).

2.2. RNA sample preparation

X. laevis were surgically dissected to obtain various tissues for total RNA extraction. Total RNA was extracted from those tissues with easy-BLUE™ (iNtRON Biotechnology) by methods established in our laboratory. Extracted total RNA was digested with RNase-free DNase I (Invitrogen) to avoid any contamination of genomic DNA.

2.3. In silico search of expressed sequence tags (EST) database and analysis

To sort the target cDNA sequence, we queried mouse TMEM16A cDNA sequences with the National Center for Biotechnology Information–Basic Local Alignment Search Tool (NCBI–BLAST) sever as to whether unknown cDNA homologous to mouse anoctamin (mTMEM16A) existed in the *X. laevis* expressed sequence tags (EST) database. *X. laevis* cDNA sequences showing appropriate homology (50–70%) were selected as candidates for the new anoctamin gene family. A small cDNA sequence (BC_094127) in the EST database was regarded as putative anoctamin compared to mouse TMEM16A. GENETYX® software (GENETYX, Tokyo, Japan) was employed for alignment of sequence homology with cDNA and amino acids.

2.4. Gene cloning of new X. laevis anoctamin (xANO2)

To obtain the first strand of cDNA, a reverse transcription (RT) reaction was performed with reverse transcriptase (SuperScript® III, Invitrogen; iScript™, BIO-RAD) and either random primer or Oligo-(dT) adaptor primer (Fig. 1A). The rapid amplification of cDNA ends (RACE) method was used with gene specific primers and linker primers. In order to obtain the full-length of xANO2 cDNA, three rounds of RACE (Fig. 1A) were performed using KOD-Plus Taq polymerase (Toyobo). Specific primer sets based on the *X. laevis* EST sequence (BC_094127) were designed and are summarized in Table 1. The initial PCR was carried out in a Peltier thermal cycler PTC-200 with denaturation at 94 °C for 1 min, followed by 20–25 cycles of 94 °C for 30 s, 60–62 °C for 30 s, and 68 °C for 1 min 50 s ~2 min 15 s. Amplified PCR products were purified through Sephacryl® S-400 resin and a spin column (PROBER, iNtRON Biotechnology) and then 1/50 of the first PCR product was used as a template for the second PCR which was also carried out in a Peltier thermal cycler PTC-200 with initial denaturation at 94 °C for 1 min, followed by 30 cycles of 94 °C for 30 s, 60–62 °C for 30 s, and 68 °C for 1 min 50 s ~2 min 10 s. A third PCR was performed with initial denaturation at 94 °C for 1 min, followed by 30 cycles of 94 °C for 30 s, 62 °C for 30 s, and 68 °C for 2 min 10 s. The gene specific primer sets (outer; AN13–AN17, inner; AN14–AN16) for full length cDNA were designed from the three cDNA fragments to avoid unspecific PCR products (Table 1). Finally, the full length of xANO2 cDNA was amplified by two rounds of nested PCR using KOD-Plus Taq polymerase (Toyobo). The nested PCR products were tailed with poly (A) and then inserted into TA cloning vector, pGEM-T Easy (Promega). The subcloned plasmid carrying xANO2 cDNA was prepared with a

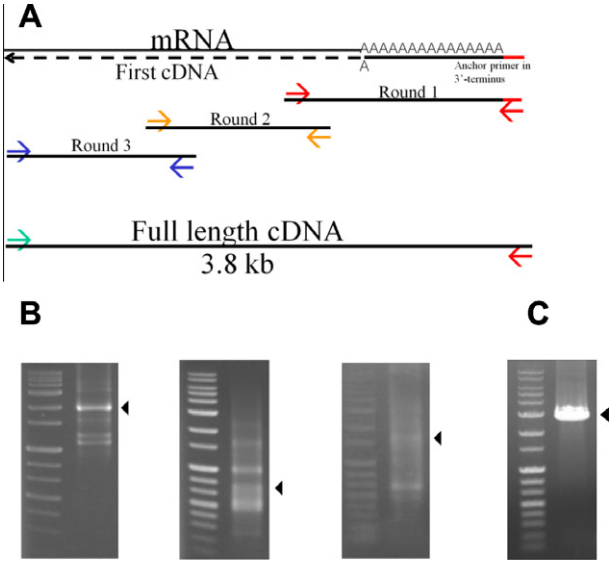

Fig. 1. Construction strategy of full-length cDNA. (A) To obtain the full length of xANO2 cDNA, three rounds of PCR were carried out under appropriate conditions. Initial cDNA (dotted line) and PCR products (thick line) are depicted with black lines. 3′-RACE products are represented as Round 1 and 5′-RACE products are represented as Round 2 and 3. (B) PCR products of 3′-RACE (left, Round 1) and 5′-RACE (middle: Round 2, right: Round 3) were electrophoresed in a 1% agarose gel. Black arrowheads indicate the 2.0, 0.7, and 1.7 kb target products. (C) Full-length PCR product of *X. laevis* TMEM16A gene. The 3012 base pair (bp) cDNA (xTMEM16A) was amplified by gene specific primers: CAN3 and CAN5.

Table 1
3′-RACE; AN3 and AN4 Round 1 in Fig. 1A. 5′-RACE; AN5, AN6 and AN7 for Round 2 and AN10 and AN11 for Round 3 in Fig. 1A. Full length PCR; AN13, AN14, AN16, AN17, ANotI and AKpnI for xANO2, CAN3 and CAN5 for xTMEM16A. RT and real-time PCR; AN16, AN17 and AN19 for xANO2, C1 and C2 for xTMEM16A, XHRMbA1 and XbA3 for β-actin.

Primer	Sequence
AN3	5′-GTGGCCTTCTTTAAGGGCAGG-3′
AN4	5′-GTTGGACGGCCTGGAGATTAC-3′
AN5	5′-AGAGATTGTTCTGAATCAGCTGC-3′
AN6	5′-TACTTAGCTGGATGCACAGTTCC-3′
AN7	5′-AACCACCAGGGGCACACTC-3′
AN10	5′-CAAACACAATTGCAAACGTCACA-3′
AN11	5′-CCACCATATTTGTTAGATAAGCC-3′
AN13	5′-ATTTACAGACGCTGCATGCG-3′
AN14	5′-CATTCTTCTGAGCCCACAGC-3′
AN16	5′-ACTGTCCAGTACGGACAGTG-3′
AN17	5′-AACCTGTTAACACAGCCTCG-3′
AN19	5′-CTTTACTGGACACGTCTGTG-3′
C1	5′-CTACCAAGCACAGTTTGAAG-3′
C2	5′-ATGGACAGCATTGGCTTAGC-3′
CAN3	5′-atagaaTTCACCGTTCCTTGCGCTG-3′
CAN5	5′-aatctcgAGCCTTAAACTGTCCTGCAC-3′
ANotI	5′-aaagcggccgcAATCAAACTATGTAAATTC-3′
AKpnI	5′-ataggtacCATTCTTCTGAGCCCACAGC-3′
XHRMbA1	5′-TGTTACCCAGATTAGGGTTGCTGGG-3′
XbA3	5′-CCAATGATGAAGAAGAGGCAG-3′

DNA-spin™ Plasmid DNA Extraction Kit (iNtRON Biotechnology) for sequence determination. The nucleotide sequence was confirmed with an ABI PRISM® System (model 377).

2.5. Reverse transcription polymerase chain reaction (RT-PCR) and quantitative PCR analysis

Total RNA from *X. laevis* tissues was used in RT-PCR to determine the expression level of each sample. A total of nine types of tissues were employed: brain, heart, lung, liver, small intestine, colon, kidney, spleen, and oocytes. One round of PCR was performed using i-StarTaq™ Polymerase (iNtRON Biotechnology), gene specific primers, AN19 and AN16, C1 and C2, and internal control primers, XHRMbA1 and XbA3. The process utilized for gene specific amplification was as described in our previous report [8]. Analysis of the relative ratios of anoctamins was performed to compare expression levels of each tissue.

The nine independent cDNAs mentioned above were also used to analyze the expression level of each tissue and confirm the result of RT-PCR. To maintain consistency, nine cDNAs from RT-PCR were used in the next experiment. A CHROMO4™ (BIO-RAD) real-time PCR system was used for analysis. Real-time PCR was performed using DyNAmo™ Flash® SYBR Green qPCR Kits (Finnzymes) with gene specific primers, AN19 and AN16, C1 and C2, and internal control primers, XHRMbA1 and XbA3 according to the following conditions: a pre-denaturation step at 95 °C for 7 min, 50 cycles of 95 °C for 15 s, 62 °C for 20 s, 72 °C 20 s, a final extension step at 72 °C for 5 min, and analysis of the melting curve from 65 to 95 °C.

2.6. Heterologous expression of anoctamins in HEK293T cells and whole-cell recordings

To express the cloned xANO2 gene, the full-length of xANO2 cDNA was re-amplified with KOD-Plus Taq polymerase and the *Kpn* I, *Not* I site-attached AKpnI and ANotI primers. In addition, the *X. laevis* TMEM16A gene was amplified from the plasmid provided by Jan laboratory using gene specific primers: *Eco*R I, *Xho* I site-attached CAN3 and CAN5 (Table 1). The amplified whole cDNAs were digested by restriction enzymes and independently inserted into pcDNA3.1$^+$ vectors (Invitrogen). The sequences of pcDNA3.1$^+$ harboring the anoctamin plasmids were confirmed by sequencing, and prepared by Plasmid Midi Kit (Qiagen). The following experimental procedures were performed by the same protocol for heterologous expression analysis. HEK293T cells were transfected with the anoctamin expression plasmids mixed with EGFP plasmid at a 10:1 ratio using Effectene (Qiagen) at 1 μg of DNA per 35-mm culture dish. The EGFP plasmid alone (100 ng) was used as a transfection control. Approximately 24 h after transfection, whole-cell recordings were performed on single isolated green cells identified under a fluorescence microscope. To activate xANO2 directly, we applied high Ca^{2+}-containing intracellular patch pipette solution to xANO2-expressing HEK293T cells, which contained the following: 146 mM CsCl, 5 mM (Ca^{2+})–EGTA–N-methyl-D-glucamine (NMDG), 2 mM $MgCl_2$, 8 mM HEPES, and 10 mM sucrose, at pH 7.3, adjusted with NMDG. Free Ca^{2+} concentration was estimated to be 4.5 μM [17]. The extracellular solution contained the following: 150 mM NaCl, 10 mM HEPES, 3 mM KCl, 2 mM $CaCl_2$, 2 mM $MgCl_2$, and 5.5 mM glucose, at pH 7.3 adjusted with NaOH (~320 mOsm). Current–voltage curves were established by applying 500 ms duration voltage ramps from −100 to +100 mV. Data were acquired with an Axopatch 200A amplifier controlled by Clampex 9.2 via a Digidata 1322A data acquisition system (Molecular Devices).

3. Results

3.1. Gene isolation of xANO2 and xTMEM16A

According to the analysis described in Section 2, a partial cDNA (BC_094127) was found and selected by alignment of mTMEM16A (mouse anoctamin) sequences as the query sequence (data not shown). The aa sequence deduced from partial cDNA showed about 80% homology.

RT-PCR was performed to obtain first strand cDNA (Fig. 1). The full-length of xANO2 cDNA was cloned by RACE as mentioned in Section 2. As shown in Fig. 1, xANO2 contains three fragments. Using AN4-adapter, linker-AN7, and linker-AN11 primer sets, fragment sizes were 1980 base pair (bp), 702, and 1603 bp, respectively. The full length of xANO2 cDNA was successfully amplified by two rounds of PCR as described in Section 2. Following subcloning into pGEM-T Easy Vector (Promega, USA), the whole sequence was confirmed, and two random recombinants were selected as final xANO2 clones which were consistent with partial cDNA. In addition, xTMEM16A cDNA was amplified as described in Section 2.6.

As a result, the full-length 3884 bp xANO2 and 3012 bp xTMEM16A coding sequences were cloned (Fig. 1). That cDNA also contains a short 5′- and a 3′-untranslated region as well as a poly $(A)^n$ tail. This sequence was registered as xANO2 gene in the DNA Data Bank of Japan (DDBJ) (GenBank, Accession No. AB599713).

3.2. Primary structure analysis

The sequence analysis of the full-length xANO2 gene revealed a single large open reading frame (ORF), along with short 5- and 3-untranslated sequences (UTRs). The xANO2 primary sequence consisted of 980 amino acids.

The xANO2 aa sequence was compared with mouse and frog TMEM16A to determine whether or not there was significant homology. The ORF of xANO2 showed 76% and 92% identity overall to those of mANO1 and xANO1 (xTMEM16A), respectively. However, the aa sequence similarity of xANO2 in the N-terminal region was very low compared to xTMEM16A (Fig. 2A). Based on the overall significant homology exhibited it was regarded as a new anoctamin family member. Also, xANO2 included multiple consensus sites of N-linked glycosylation, phosphorylation by protein kinase C, cAMP- and cGMP-dependent protein kinase, and casein kinase II.

In hydropathy analysis of the full-length xANO2 using the Kyte–Doolittle method on the GENETYX program, the ORF in xANO2 showed eight potential transmembrane (TM)-spanning domains and one reentrant loop (Fig. 2B). The primary structure of xTMEM16A [1] was also deduced and analyzed by the same method as previously described. The hydropathy plot of xTMEM16A was absolutely the same as the overall region of xANO2 except for a short range of amino terminus (Fig. 2B). As mentioned, the results of hydropathy analysis for xANO2 showed overall consistency with xTMEM16A.

3.3. Gene expression profiles in tissue distribution

To analyze the gene expression levels of xANO2 and xTMEM16A, we performed 38 repeats of RT-PCR with nine different *Xenopus* tissue samples including brain, heart, lung, liver, small intestine, colon, kidney, spleen, and oocytes. According to RT-PCR analysis, xANO2 was ubiquitously expressed in various *X. laevis* tissues (Fig. 3). In particular, expression levels in some tissues, including lung, liver, and spleen, were higher than the others (Fig. 3A and C). xTMEM16A was also expressed in some tissues, including oocyte, spleen, intestines, lung and liver. Interestingly, it was almost

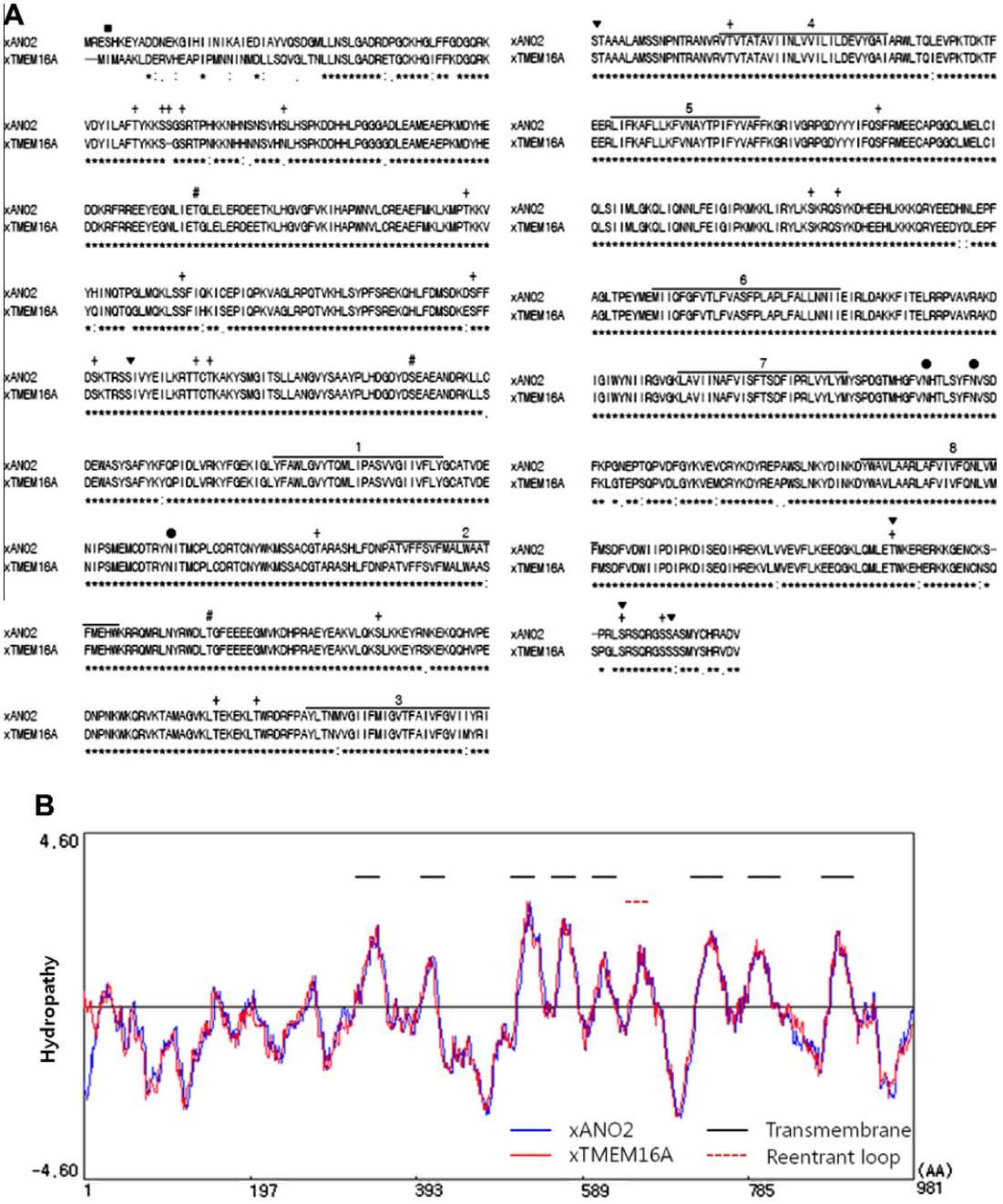

Fig. 2. Primary structure analysis of *X. laevis* anoctamins. (A) Amino acid (aa) alignment was deduced by querying the xANO2 aa sequence using GENETYX. The aa homology is indicated as follows: identical (asterisk), similar (dot). The putative transmembrane regions are marked by an upper line. Consensus sites are marked for N-linked glycosylation (●), phosphorylation by PKA (▼), PKC (+), PKG (■), casein II (#). (B) Hydrophobicity plots (Kyte–Doolittle analysis) of the anoctamin aa sequences. Both hydropathy plots were absolutely consistent in the overall region except for a short range at the amino terminus. The hydropathy plots were analyzed using an analysis window of 17 residues, and then overlapped. Hydrophobic domains are given as positive values. The proposed TM segments and reentrant loop are indicated by horizontal lines and dotted line, respectively.

not detected in brain and heart compared to the dominant expression in oocytes (Fig. 3A and C).

To confirm the RT-PCR results, 50 cycles of real-time PCR were performed using the same samples. The data of real-time PCR showed that xANO2 was significantly expressed in the liver. The results ranked in expression order are as follow: liver > kidney > sm.int = spleen > oocyte > colon = lung > brain > heart. In contrast, according to the real-time PCR results, xTMEM16A expression was detected most dominantly in oocytes (Fig. 3B).

These results showed slightly different expression levels, but were mostly consistent with the RT-PCR results (Fig. 3). Melting curve steps were performed to confirm the exact amplification of products.

3.4. Heterologous expression of xANO2 and xTMEM16A in HEK293 cells

The functional expression of xANO2 and xTMEM16A as anion channels were investigated by transfection into HEK293T cells with corresponding cDNA. Ca^{2+} activated anion currents were measured by whole cell patch-clamp recordings using patch pipette internal solution containing 4.5 μM Ca^{2+}. In the current–voltage

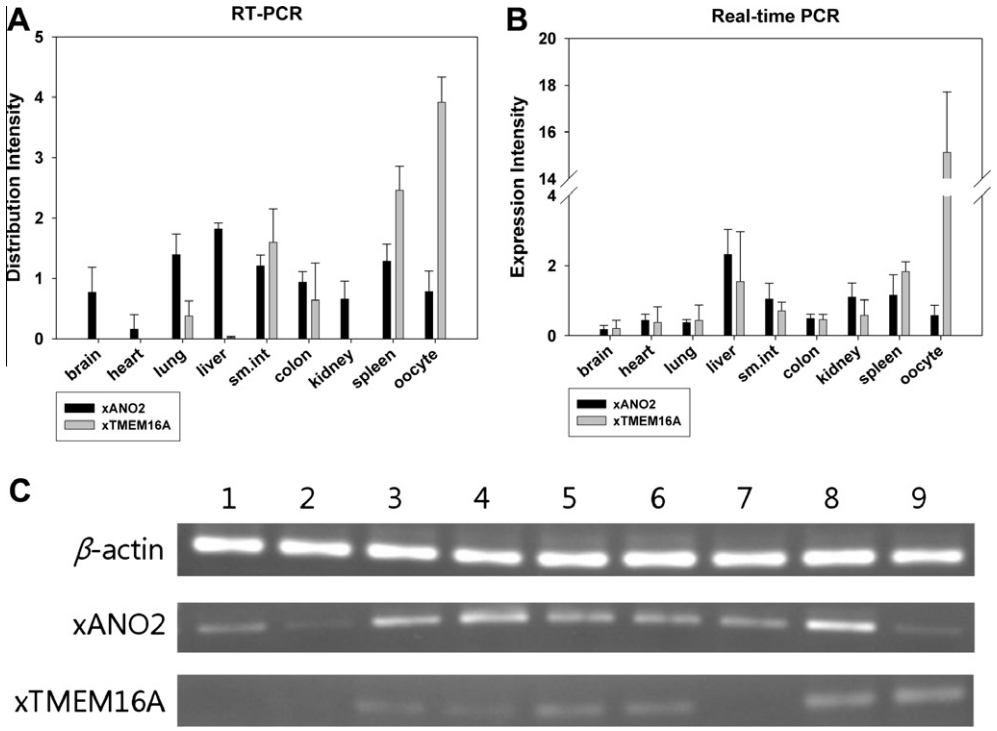

Fig. 3. Comparison of anoctamin expression in *X. laevis* by reverse transcriptase (RT)-PCR and real-time PCR. Each expression level of anoctamins was normalized with β-actin used as internal control. (A) Bar graphs of RT-PCR. One round of PCR was carried out with 38 repeats to determine the specific products of xANO2, xTMEM16A, and β-actin gene. Each specific product of xANO2, xTMEM16A, and β-actin gene was amplified by RT-PCR. The β-actin gene was used as an internal control. Lanes 1–9 represent brain, heart, lung, liver, small intestine, colon, kidney, spleen and oocyte, respectively. (B) Quantitative histogram of real-time PCR. Real-time PCR was carried out with 50 repeats for quantitative analysis for anoctamin expression in *X. laevis* tissues. (C) Tissue distributions of anoctamin mRNA expression. Quantitation of anoctamin is shown as a bar graph compared to RT-PCR.

relationship, HEK293T cells showed anion currents with voltage-dependent behavior that was significantly higher than that of mock control cells (current amplitude from V_h = +100 to −100 mV; 2655.6 ± 389.8 pA [n = 9] for xANO2 expression with high Ca^{2+} and 71.6 ± 12.3 pA [n = 6] for mock-transfected cell with high Ca^{2+}; $^{***}p < 0.0001$ vs. xANO2 expression in high Ca^{2+} group; two tailed t-test, for same behavior in TMEM16A; 4450.6 ± 403.6 pA [n = 13] for xTMEM16A expression with high Ca^{2+} and 80.7 ± 13.4 pA [n = 7] for mock-transfected cell with high Ca^{2+}; $^{***}p < 0.0001$ vs. xTMEM16A expression in high Ca^{2+} group) (Fig. 4A and C). In xANO2-transfected cells, the reversal potential of the membrane current was close to 0 mV, which is consistent with an anion-selective channel. We also used a chloride channel blocker, niflumic acid (NFA), which is a strong blocker of the endogenous Ca^{2+}-activated Cl^- current in *Xenopus* oocytes [18]. In the presence of 100 μM NFA, the Cl^- currents induced by anoctamin transfection were mostly inhibited (current amplitude from V_h = +100 to 100 mV; 502.7 ± 117.5 pA [n = 8], $^{***}p < 0.0001$ vs. xANO2 expression in high Ca^{2+} group; two tailed t-test; 1040.5 ± 250.4 pA [n = 8], $^{***}p < 0.0001$ vs. xTMEM16A expression in high Ca^{2+} group; two tailed t-test) (Fig. 4B and D). During the inhibition effects of NFA, the Cl^- currents were significantly diminished to one-fifth in xANO2 compared to one-fourth in xTMEM16A (Fig. 4E). These data suggest that heterologously expressed xANO2 encodes a Ca^{2+}-activated anion channel similar to xTMEM16A.

4. Discussion

The animal CLCAs have been mainly studied in mammals including human, mouse, rat, porcine, and bovine species [4–9]. TMEM16A (xANO1) is a member of the TMEM16 family related to the association of CLCA expression as a Ca^{2+}-activated chloride channel subunit [1]. Among the mouse mTMEM16 family gene, mTMEM16A expressed in the airway and foregut epithelia is an essential factor for survival [17]. Considering the influence on multiple cancers associated with poor prognosis by amplification of human TMEM16A, TMEM16A as a CLCA modulator might be a tool for cancer therapy [19–21].

We have been searching for new CLCAs in *X. laevis* using various *X. laevis* tissues. Here, we report on the isolation of xANO2 as a CaCC in *X. laevis*. We have successfully completed cloning of xANO2 which consists of 3884 bp cDNA from *X. laevis*. Even though xANO2 shows very high homology to *Xenopus* TMEM16A, it was not identical in its amino terminus (Fig. 2A and B). This unique amino terminus sequence of xANO2 compared to xTMEM16A is an interesting finding.

Despite the ubiquitous expression of xANO2 in *Xenopus* tissues, expression levels in liver, spleen, and lung showed little difference. It is presumed that *Xenopus* ANO1 (xTMEM16A) [1] and xANO2 have common characteristics expressed ubiquitously in various tissues. RT-PCR analysis confirmed the other supportive data showing ubiquitous expression in different tissues. Despite the ubiquitous expression of xANO2 and xTMEM16A, they have distinct patterns in some tissues such as brain and oocytes. Using HEK293T cells, we successfully expressed functional xANO2, as shown by observation of currents in xANO2 + EGFP co-transfected cells but not in cells transfected with EGFP alone. The currents evoked when the pipette solution contained Ca^{2+} were significantly inhibited by NFA, a Cl^- channel blocker. Interestingly, xANO2 was inhibited with 100 μM NFA in contrast to our previous studies [8,22] that employed a concentration of 300 μM NFA for complete

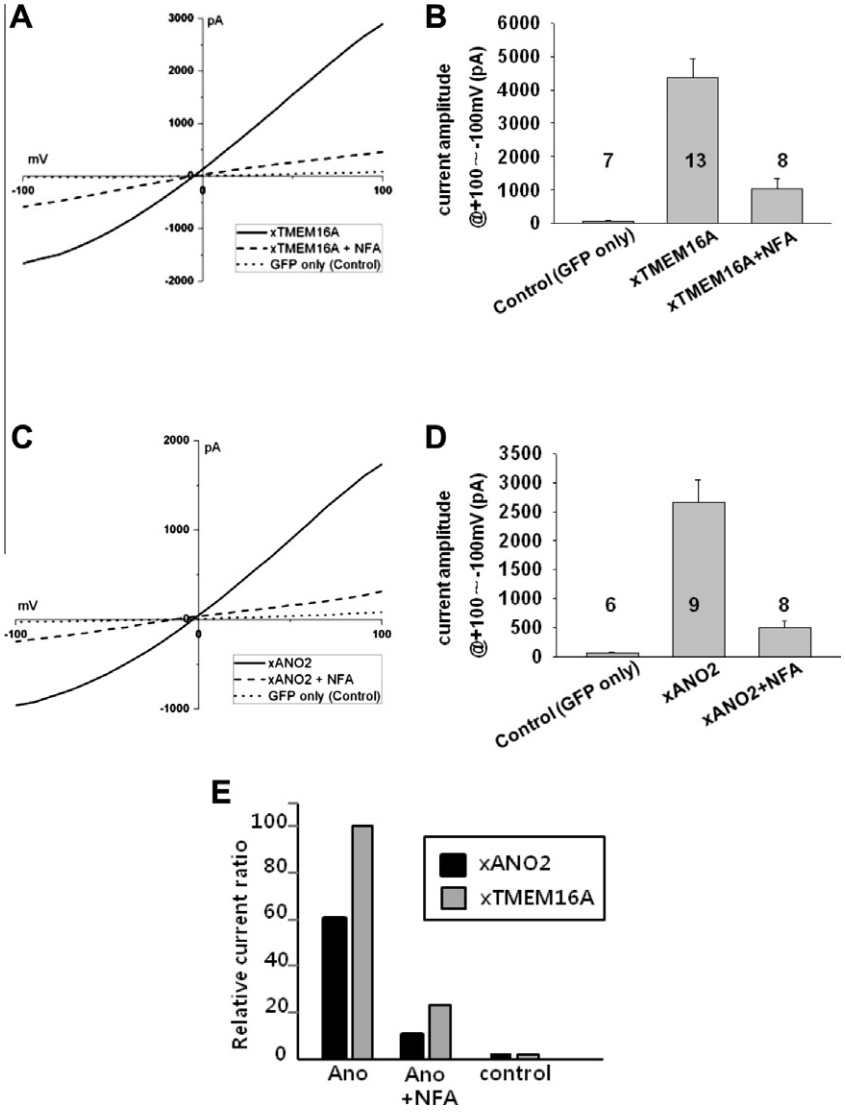

Fig. 4. xANO2 as a Ca^{2+} activated anion channel. (A and C) Representative *I–V* responses of HEK293T cells expressing xTMEM16A (A), xANO2 (C), or mock control under whole-cell patch-clamp configuration using 4.5 μM Ca^{2+}-containing patch pipette solution. (B and D) Bar graph showing summary of current amplitudes recorded from a holding potential of −100 to +100 mV (mean ± SEM). The anion channel blocker niflumic acid (NFA; 100 μM) was preincubated with cells for 10 min. Number of determinations are indicated on the bar graph. $^{***}p < 0.0001$ vs. anoctamin-expressing cells with 4.5 μM Ca^{2+} pipette solution, two tailed *t*-test. Each B and D bar graphs is depicted for A and C *I–V* responses. (E) Relative ratios of current amplitude. Each bar was depicted by the calculated percentage for xTMEM16A as full positive current.

inhibition. Actually, it appeared that the inhibition ratio for xANO2 was more significant than xTMEM16A (Fig. 4E). These results indicate that xANO2 is more sensitive to NFA when compared to other types of CLCAs previous studied [8].

In summary, we identified a new xANO encoding the *Xenopus* TMEM16, xANO2, as a CaCC. Further physiological and biochemical studies may clarify the gene functions of the CLCA family including TMEM16A. Also, additional research is required on CaCC family members in different organisms.

Acknowledgments

This research was supported by funding to S.M. Jeong from a Korean Research Foundation Grant by the Ministry of Education and Human Resources Development (KRF-313-2007-2-E00519) and the Brain Korea 21 Project. This research was supported by the Technology Development Program for Agriculture and Forestry (2010-A008-0034) from the Ministry for Food, Agriculture, Forestry and Fisheries, Republic of Korea. The company grant was supported by Takara Korea. *Xenopus laevis* was kindly provided by Dr. Nah S.Y. (Konkuk University, Seoul, Korea).

References

[1] B.C. Schroeder, T. Cheng, Y.N. Jan, L.Y. Jan, Expression cloning of TMEM16A as a calcium-activated chloride channel subunit, Cell 134 (2008) 1019–1029.

[2] A. Caputo, F. Caci, L. Ferrera, et al., TMEM16A, a membrane protein associated with calcium-dependent chloride channel activity, Science 322 (2008) 590–594.

[3] F. Huang, J.R. Rock, B.D. Harfe, et al., Studies on expression and function of the TMEM16A calcium-activated chloride channel, Proc. Natl. Acad. Sci. 106 (2009) 21413–21418.

[4] Y.D. Yang, H. Cho, J.Y. Koo, et al., TMEM16A confers receptor-activated calcium-dependent chloride conductance, Nature 455 (2008) 1210–1215.

[5] M. Agnel, T. Vermat, J.M. Culouscou, Identification of three novel members of the calcium-dependent chloride channel (CaCC) family predominantly expressed in the digestive tract and trachea, FEBS Lett. 455 (1999) 295–301.

[6] R. Gandhi, R.C. Elble, A.D. Gruber, et al., Molecular and functional characterization of a calcium-sensitive chloride channel from mouse lung, J. Biol. Chem. 273 (1998) 32096–32101.

[7] S.R. Evans, W.B. Thoreson, C.L. Beck, Molecular and functional analyses of two new calcium-activated chloride channel family members from mouse eye and intestine, J. Biol. Chem. 279 (2004) 41792–41800.
[8] S.M. Jeong, H.K. Park, I.S. Yoon, et al., Cloning and expression of Ca^{2+} activated chloride channel from rat brain, Biochem. Biophys. Res. Commun. 334 (2005) 569–576.
[9] K.J. Gaspar, K.J. Racette, J.R. Gordon, et al., Cloning a chloride conductance mediator from the apical membrane of porcine ileal enterocytes, Physiol. Genomics 3 (2000) 101–111.
[10] S.A. Cunningham, M.S. Awayda, J.K. Bubien, et al., Cloning of an epithelial chloride channel from bovine trachea, J. Biol. Chem. 270 (1995) 31016–31026.
[11] L.H. Clapp, J.L. Turner, R.Z. Kozlowski, Ca(2+)-activated Cl^- currents in pulmonary arterial myocytes, Am. J. Physiol. 270 (1996) H1577–H1584.
[12] Y. Hirakawa, M. Gericke, R.A. Cohen, et al., Ca(2+)-dependent Cl(−) channels in mouse and rabbit aortic smooth muscle cells: regulation by intracellular Ca(2+) and NO, Am. J. Physiol. 277 (1999) H1732–H1744.
[13] S.J. Huang, W.O. Fu, Y.W. Chung, et al., Properties of cAMP-dependent and Ca(2+)-dependent whole cell Cl^- conductances in rat epididymal cells, Am. J. Physiol. 264 (1993) C794–C802.
[14] M.E. Loewen, G.W. Forsyth, Structure and function of CLCA proteins, Physiol. Rev. 85 (2005) 1061–1092.
[15] R. Tarran, B. Button, R.C. Boucher, Regulation of normal and cystic fibrosis airway surface liquid volume by phasic shear stress, Annu. Rev. Physiol. 68 (2006) 543–561.
[16] J.R. Rock, C.R. Futtner, B.D. Harfe, The transmembrane protein TMEM16A is required for normal development of the murine trachea, Dev. Biol. 321 (2008) 141–149.
[17] C.H. Hartzell, I. Putzier, J. Arreola, Calcium-activated chloride channels, Annu. Rev. Physiol. 67 (2005) 719–758.
[18] S. Choi, S.H. Rho, S.Y. Jung, et al., A novel activation of Ca^{2+}-activated Cl^- channel in *Xenopus* oocytes by ginseng saponins: evidence for the involvement of phospholipase C and intracellular Ca^{2+} mobilization, Br. J. Pharmacol. 132 (2001) 641–648.
[19] A. Carles, R. Millon, A. Cromer, et al., Head and neck squamous cell carcinoma transcriptome analysis by comprehensive validated differential display, Oncogene 25 (2006) 1821–1831.
[20] X. Huang, T.E. Godfrey, W.E. Gooding, et al., Comprehensive genome and transcriptome analysis of the 11q13 amplicon in human oral cancer and synteny to the 7F5 amplicon in murine oval carcinoma, Genes Chromosomes Cancer 45 (2006) 1058–1069.
[21] R.B. West, C.L. Corless, X. Chen, et al., The novel marker, DOG1, is expressed ubiquitously in gastrointestinal stromal tumors irrepective of KIT or PDGFRA mutation status, Am. J. Pathol. 165 (2004) 107–113.
[22] I.S. Yoon, S.M. Jeong, S.N. Lee, et al., Cloning and heterologous expression of a Ca^{2+} activated chloride channel isoform from rat brain, Biol. Pharm. Bull. 29 (2006) 29 2168–2173.